# THE EFFECT OF POSS-POLYIMIDE FILM'S NANOSTRUCTURE ON ITS MECHANICAL PROPERTIES

**R. Verker [1,2], E. Grossman [1], I. Gouzman [1], N. Eliaz [2]**

[1] *Space Environment Section, Soreq NRC, Yavne 81800, Israel, +972-8-9434397, rverker@soreq.gov.il*
[2] *School of Mechanical Engineering, Tel-Aviv University, Ramat Aviv, Tel-Aviv 69978, Israel*

## ABSTRACT

The amount of hypervelocity low-Earth orbital debris has increased dramatically in recent years, leading to an increase in the number of hypervelocity impacts on satellite external surfaces. A promising approach toward the production of a low-Earth orbit (LEO) material, which can survive hypervelocity impacts, is based on a nanocomposite comprised of inorganic Polyhedral Oligomeric Silsesquioxane (POSS) molecules and an organic Polyimide (PI) matrix. POSS-PI shows significant enhancement in withstanding the space environment, especially in terms of atomic oxygen (AO) erosion resistance. Previous work also showed that POSS-PI films that were subjected to ground simulated hypervelocity orbital debris impacts and AO exposure revealed enhanced durability.

In this work, a laser-driven flyer system was used to accelerate aluminum flyers to impact velocities of up to 3 km/s at temperatures ranging from –60 to +100°C. The ultrahigh velocity impacts of the POSS-containing PI films were characterized by a more brittle appearance compared to pure PI films, raising a need for a fundamental mechanical properties study.

POSS-PI films were analyzed for chemical and morphological characteristics. The curing process of PI and POSS-PI, monitored using Fourier Transform Infrared (FTIR) spectroscopy, showed no evidence of chemical reaction between the POSS and the PI. However, the results indicated on a POSS-POSS condensation reaction. Surface morphology examination, obtained by Atomic Force Microscopy (AFM), showed formation of aggregates, the size and density of which were affected by the POSS content. Intermolecular POSS-POSS condensation reaction was identified as a key factor, affecting the nanocomposite mechanical properties via formation of aggregates. The amount and density of these aggregates were shown to be composition dependent. A model based on formation and coalescence of voids during tensile tests was suggested to explain the effect of the POSS content on the POSS-PI mechanical response.

## 1. INTRODUCTION

Nowadays, numerous satellites are being launched into low Earth orbit (LEO) altitudes, ranging from 200 to 1000 km. The degrading environment in LEO includes atomic oxygen (AO), ultraviolet (UV) and ionizing radiation, ultrahigh vacuum (UHV), thermal cycling, and ultrahigh velocity micrometeoroids and orbital debris [1-3]. The breakup of satellites, either deliberately or accidentally, leads to an increasing amount of orbital debris, which further leads to additional events of ultrahigh velocity impacts onto satellites' external surfaces. Polyimides (PIs), such as Kapton®, are used extensively in spacecraft external surfaces as thermal blankets, in solar arrays, and space inflatable structures [4, 5]. $SiO_2$ coatings have been shown to provide a sufficient protection against AO attack; however, inherent or hypervelocity debris-induced defects in the coating will permit AO penetration and attack of the underlying polymer [6]. Developing materials which can sustain such impacts and still function under the harsh conditions of the LEO environment is therefore needed. In the past two decades, polymer nanocomposites have attracted a great deal of research interest because, if well dispersed, they may exhibit substantially improved physical and mechanical properties. Polymer-based nanocomposites are a novel class of materials that are reinforced by one or more types of fillers, of which at least one dimension of the dispersed particles in the polymer matrix is on the nanometer scale [7].

A promising approach toward the production of LEO survivable polymer-based nanocomposites is incorporation of inorganic Polyhedral Oligomeric Silsesquioxane (POSS) into the organic polymeric chains [8-10]. POSS-containing PIs have shown significantly lower AO erosion yields than pure PI, since AO irradiation results in formation of $SiO_2$ passivation layer, which protects the underlying polymer from further AO attack [8].

In previous studies, PI and POSS-PI nanocomposite films were exposed to hypervelocity impacts at room temperature and subsequently to air RF plasma (which simulates AO environment) [11]. As a result, an impacted PI film eroded one order of magnitude faster than impacted 15 wt.% POSS-PI. The low erosion rate of the impacted 15 wt.% POSS-PI film was attributed to both mechanical (i.e. no residual tensile stresses) and chemical (i.e. formation of an oxide passivation layer) aspects [11].

The different response of PI and POSS-PI to hypervelocity impacts performed at room temperature and subsequent AO exposure [11] have initiated a fundamental study of the mechanical properties, surface morphology and chemical composition of these materials. Due to thermal cycles hypervelocity impacts take place in LEO at temperatures of -60 up to +100°C. Therefore, in the present work, tensile tests, FTIR analysis and surface morphology characterization are used to explain the effect of the POSS content on the mechanical properties and the fracture mechanism during the hypervelocity impacts at various temperatures.

## 2. EXPERIMENTAL

### 2.1. <u>Materials and film preparation</u>

The materials studied in this work were blends of oxydianiline-pyromellitic dianhydryde (ODA-PMDA) PI (Pyre-M.L. RC-5019 by Industrial Summit Technology, Co.) and trisilanolphenyl (TSP)-POSS (Hybrid Plastics, Inc.). Fig. 1a and 1b show a schematic presentation of the PMDA-ODA PI monomer and trisilanolphenyl-POSS molecule, respectively.

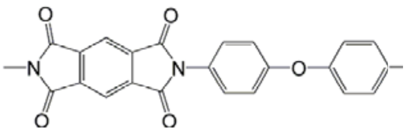

**(a)**

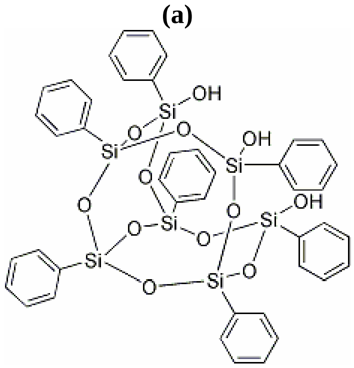

**(b)**

Fig. 1. Schematic presentation of PMDA-ODA PI monomer (a) and TSP-POSS molecule (b).

Samples were produced in the form of thin films, 25–30 µm thick. Films with POSS contents of 0 (PI) and 15 wt.%. POSS were produced using a bench-scale process of casting and curing a pre-mixed solution of polyamic acid and POSS in N-methyl-pyrrolidone (NMP) solvent. The curing of the pre-mixed solution is based on a process developed by DuPont, Inc. After casting the pre-mixed solution into a glass mold, the samples were heated to 200ºC in air, at a heating rate of 4ºC/min and held for a period of 30 min. In a second temperature cycle, the samples were heated to 350ºC in the presence of pure nitrogen, at a heating rate of 2ºC/min, and held for a period of 60 min. In order to minimize residual stresses, the final stage was slow cooling at a rate of 2ºC/min, down to room temperature [12]. At room temperature, the PI and POSS-PI films were peeled off the glass mold.

### 2.2. <u>Laser-driven flyer method</u>

A laser-driven flyer (LDF) method was used for generating simulated space hypervelocity debris [13-15]. The LDF system is based on a high-power titanium:sapphire laser (Thales Laser) with a wavelength of 810 nm, pulse energies from 250 to 710 mJ, and a pulse length of 300 ps. The laser beam is guided into a vacuum chamber operating at a base pressure of 65 mTorr. Before entering the chamber, the beam passes through a focusing lens. The beam target is a 12 µm thick pure aluminum foil bonded to a BK7 glass by means of a field-assisted diffusion bonding process. The beam passes through the glass without interacting with it, until it hits the aluminum/glass interface. At the interface, a high-temperature, high-pressure plasma is formed, which then expands perpendicularly to the foil. The expanding plasma induces a series of shock and rarefaction waves, forming a spall [16]. A pressure gradient between the high-pressure plasma on one side of the spall, and the vacuum on the other side of the spall, causes the spalled layer to accelerate, resulting in an aluminum layer, 1 mm in diameter, flying away at an ultrahigh velocity of up to 3 km/s. The aluminum layer is accelerated not as one flyer, but rather as small particles, 10–100 µm in size, all traveling at ultrahigh velocities [17]. The LDF system's sample holder is capable of changing the sample's temperature in a wide range from -60ºC to +100ºC.

### 2.3. <u>Tensile tests</u>

Tensile properties of 25–30 µm POSS-PI freestanding films were measured in accordance with ASTM D882-88, at a crosshead speed of 20 mm/min. The specimens used for the tensile tests were die-cut into dog-bone shaped samples with a width of 3.5 mm in the gauge region. Tensile tests were performed using an initial distance of 43 mm between grips. The samples were tested using a universal testing machine (Instron model 1026), equipped with a load cell of 2 kg. Tensile tests were performed on five specimens of each POSS-PI composition. The highest reading at peak load of each tensile test was reported as the tensile strength. The elongation values at the breaking point were used to obtain the percentage elongation [18].

### 2.4. <u>Characterization techniques</u>

The morphology of fracture surfaces was studied using Environmental Scanning Electron Microscopes (ESEM; Models Quanta 200 and 200F from FEI). These microscopes allow characterization of degassing and non-conductive samples, such as PI and POSS-PI samples, without the need for conductive coating. FTIR spectra were obtained using Bruker Vertex 70 spectrometer. At least 32 scans at a resolution of 4 $cm^{-1}$ were performed for each sample. The surface morphology of the samples was studied using an Atomic Force Microscope (AFM, MultiMode, Nanoscope IV from Veeco).

## 3. RESULTS AND DISCUSSION

### 3.1 Hypervelocity impacts

The effect of POSS content on the extent of damage of hypervelocity impacted PI and 15 wt.% POSS-PI is demonstrated in Fig. 2. The fractures were created using flyer velocities of 2.1 (Figs. 2a and 2c) and 2.9 (Figs. 2b and 2d) km/s. Both samples had the same thickness of 26 µm.

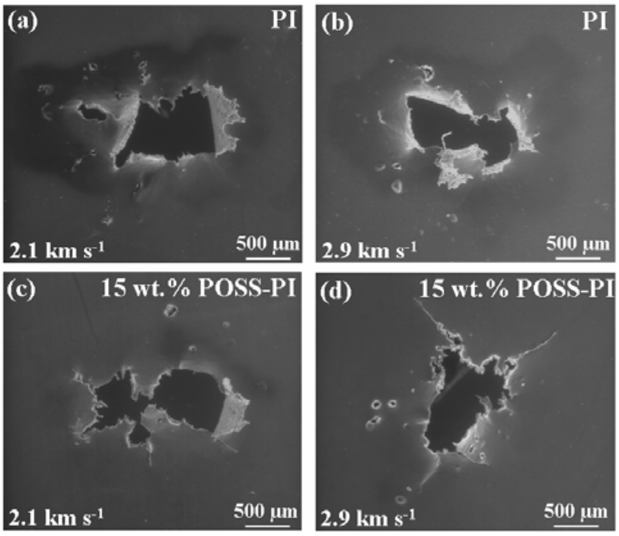


Fig. 2. ESEM images of 26 µm-thick PI (2a and 2b) and 15 wt.% POSS-PI films (2c and 2d), impacted by flyers at an equal velocity of 2.1 (2a and 2c) and 2.9 km/s (2b and 2d) aluminum flyers.

The fractography of commercial PI (Kapton-HN) film subjected to hypervelocity impacts was studied in details elsewhere [17]. The impact on Kapton-HN films introduces high temperatures ($T>T_g$) at the central impact region, and lower temperatures ($T<T_g$) at remote regions, where $T_g$ is the glass transition temperature. Consequently, the central impact region is characterized by ductile-like fracture, whereas the remote radial crack regions are characterized by a brittle-like fracture.

Considering the above variables, a comparison of the hypervelocity impacts on the PI film to that of the 15 wt.% POSS-PI film reveals that adding POSS to the PI does not change significantly the extent of damage created by the impact in terms of perforated area. The perforated area of the POSS-containing sample, due to shearing and bending of the film, is about the same as that of the PI sample, at both velocities. However, under the same impact conditions, the POSS-containing sample shows a more brittle fracture surface, via formation of radial cracking, compared to the PI sample.

The effect of the impact velocity vs. POSS content on the extent of damage of impacted POSS-PI films is also demonstrated in Fig. 2. At low impact velocity of 2.1 km/s, the PI film (Fig. 2a) is characterized by a relatively large perforated penetration hole, which was formed mainly due to bending of the film from the center of the impact, outward. The fractured surfaces of this sample are ductile, mainly due to elevated temperature that was formed during the impact.

At the same low impact velocity, the 15 wt.% POSS-PI film (Fig. 2c) is characterized by a perforated penetration hole of about the same size as the PI penetration hole. However, while some of the film segments are bended outward as in the case of PI, there are film segments that were sheared-off during the impact. The fractured surfaces of this sample are also ductile at the center. However, initiation of radial cracking is evident even at this relatively low impact velocity. During the mixed-mode impact, tensile stresses are developed parallel to the film plane. The radial cracks, which are evident on Fig. 2c, propagate perpendicular to these stresses.

At a high impact velocity of 2.9 km/s, the PI film (Fig. 2b) is characterized by a perforated penetration hole that was also formed due to bending of the film from the center of the impact, outward. It appears that PI is not greatly affected by the increase in impact velocity, and as in the low-velocity case, no radial cracks are apparent.

At the same high impact velocity, the 15 wt.% POSS-PI film (Fig. 2d) is characterized by a perforated penetration hole of about the same size as the low velocity 15 wt.% POSS-PI penetration hole. Ductile fractured surfaces and brittle radial cracks are also evident around the center of the impact point, as expected for this higher impact velocity experiment. However, the length of these radial cracks is about an order of magnitude greater compared to the low impact velocity 15 wt.% POSS-PI sample. The formation of radial cracks and, by that, the formation of higher amount of fractured surfaces in the case of the POSS-PI films, compared to the PI films, enables this class of materials to release higher amount of residual stresses, which may be formed due to the ultrahigh velocity impact.

The effect of the samples' temperature and POSS content on the extent of damage of impacted PI and POSS-PI films is demonstrated in Fig. 3. The fractures of PI and 15 wt.% POSS-PI films were created while the samples were maintained at a temperature of -60°C (Fig. 3a and 3b), RT (Figs. 3c and 3d), and 100°C (Figs. 3e and 3f). The impact velocity was not measured

during these experiments; however, according to previous measurements, it is estimated to be around 3 km/s. All samples had thickness of 26 µm.
In terms of perforated area, at temperatures of -60°C, RT and 100°C, the PI film presents similar results. At all three temperatures, the formation of perforation was due to film ripping and bending, and not film shearing. The effect of the temperature can be seen in terms of radial cracking and ductility. While at -60°C and RT small radial cracks were formed around the central impact point, at 100°C radial cracking is absent. In all three PI samples the fractured surfaces around the central impact region are ductile in nature.

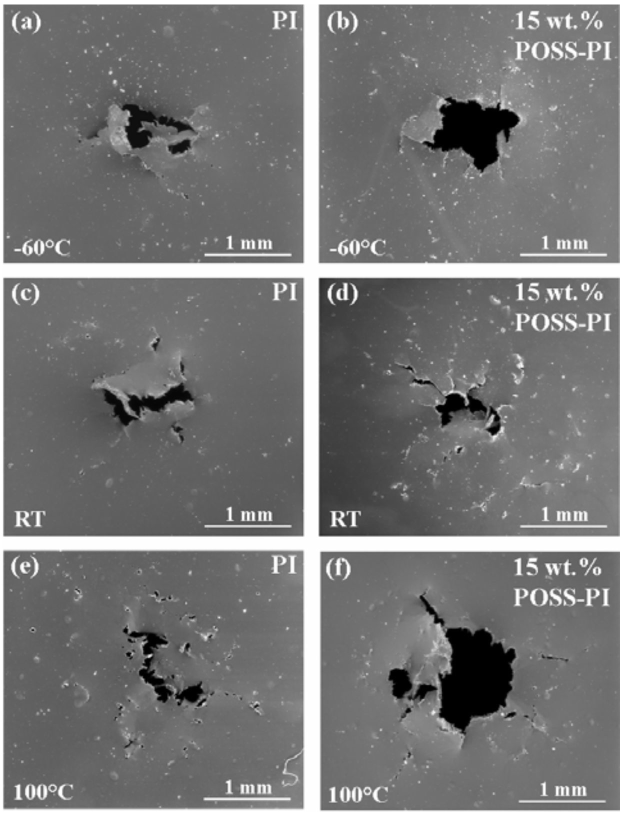

Fig. 3. ESEM images of 26 µm-thick PI (3a, 3c and 3e) and 15 wt.% POSS-PI (3b, 3d and 3f) films, maintained at temperatures of -60°C (3a and 3b), RT (3c and 3d) and 100°C (3e and 3f), impacted by an estimated hypervelocity of 3 km/s.

As mentioned before, this ductility may be attributed to the elevated temperatures which are developed during the impact. The amount of ductility of the PI sample that was maintained at 100°C (Fig. 3e) is higher compared to the two other temperatures. The higher ductility can be explained by higher mobility and elongation formed in the PI chains by the extra heat applied to the sample at 100°C and the heat formed during the hypervelocity impact. This given extra heating allowed the PI chains a higher degree of freedom in terms of chain stretching.

The fractography results of the 15 wt.% POSS-PI films are not as trivial as in the case of PI. At RT the perforated area of the 15 wt.% POSS-PI film resemble the PI perforated area. However, at -60°C and 100°C the perforated areas are much larger. At RT impact, the formation of the perforated area is due to film ripping and bending. At the extreme temperatures impacts, some bending is evident, but mostly the films were sheared during the impact, and the result is a higher perforated area.
Susceptibility of the 15 wt.% POSS-PI film to shearing at a temperature of -60°C is straightforward and can be explained by the lower degree of chain mobility. The shearing of the 15 wt.% POSS-PI film at 100°C temperature is somewhat less expected. Fig. 4 shows high-magnification ESEM images of the PI and 15 wt.% POSS-PI samples that were impacted while their temperature is maintained at 100°C. The ESEM images show the fracture surfaces at the central impact region. The difference between the two samples is clear. The fractured surface of the PI sample is ductile in nature, characterized mainly by elongated ligaments emanating from the fractured surface. The fracture surface of the 15 wt.% POSS-PI sample can be described as spongy in nature, and the existence of voids is evident. The different fractography will be discussed in Section 3.3.

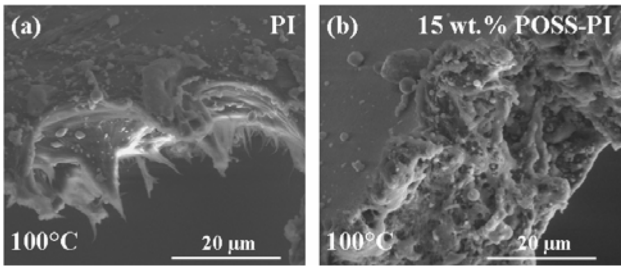

Fig. 4. High-magnification ESEM images of PI (4a) and 15 wt.% POSS-PI (4b) samples maintained at temperature of 100°C, which were impacted by ultrahigh velocity flyers.

### 3.2 POSS-PI characterization

Typical tensile stress-strain curves of PI and 15 wt.% POSS-PI are shown in Fig. 5. The PI sample (curve A) exhibits a gradual transition from elastic to plastic behavior, without a well-defined yield point. A similar behavior is observed for the 15 wt.% POSS-PI sample (curve B). The tensile strength and elongation at break of the PI are 138 MPa and 31%, respectively. Addition of 15 wt.% POSS to the PI matrix leads to reduction in toughness, resulting in low tensile strength and elongation at break of 104 MPa and 12%, respectively. The reduction in toughness of the 15 wt.% POSS-containing PI may be indicative of disruption of the polymer molecular structure [19], as will be further discussed.

Fig. 6 shows zoom-in FTIR spectra of the Si-O-Si stretching vibration region from 1200 to 1020 $cm^{-1}$ of PI, 15 wt.% POSS-PI and pure TSP-POSS, the latter serving as a reference.

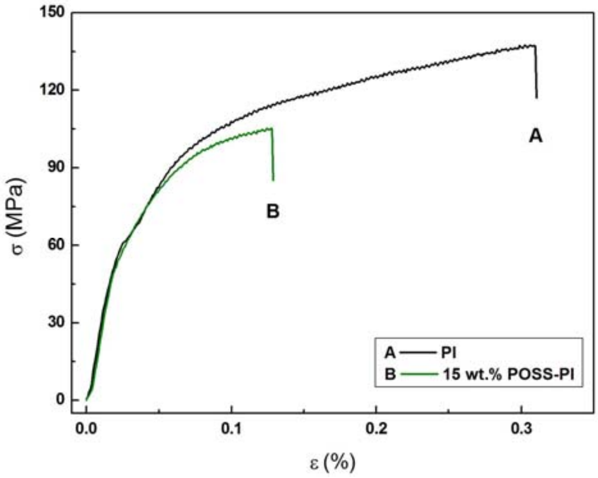


Fig. 5. Typical stress-elongation curves of PI and 15 wt.% POSS-PI films.

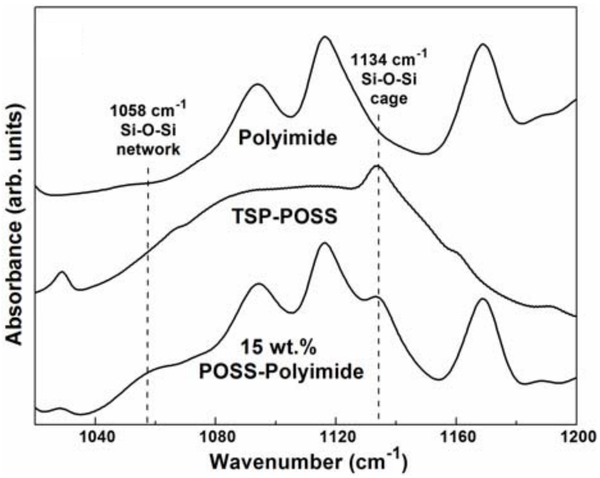


Fig. 6. Zoom-in FTIR spectra of the Si-O-Si stretching vibration region of pristine PI, TSP-POSS and 15 wt.% POSS-PI films.

The 15 wt.% POSS-PI spectrum shows two peaks at 1134 $cm^{-1}$ and at 1058 $cm^{-1}$, which are not apparent in the FTIR spectrum for PI. The peak at 1134 $cm^{-1}$ belongs to Si-O-Si cage stretching vibration. The peak at 1058 $cm^{-1}$ is attributed to Si-O-Si network stretching vibration [20]. The FTIR spectrum of TSP-POSS shows a large peak at 1134 $cm^{-1}$, which belongs to Si-O-Si cage stretching vibration. The peak at 1058 $cm^{-1}$ is an indication to a network of Si-O-Si groups, which are the result of POSS-POSS reaction via condensation. The Si-O-Si networking groups appear only in the 15 wt.% POSS-PI spectrum, which was exposed to a curing temperature of 350°C, and not in the TSP-POSS reference spectrum, which was prepared at RT. This result indicates that Si-O-Si networking forms due to the elevated temperature to which TSP-POSS was exposed during the 15 wt.% POSS-PI curing process.

POSS-POSS interaction via Si-O-Si networking or via physical aggregation is further supported by surface morphology obtained using AFM. Fig. 7 shows AFM images of pristine PI film (a) and 15 wt.% POSS-PI (b) films. The surface morphology of the PI sample is smooth, except for some scratches on the surface. The 15 wt.% POSS-PI sample reveals a rather different morphology, which is characterized mainly by the appearance of aggregates on the surface. The formation of aggregates on the surface of the POSS-PI sample is assumed to occur through migration of POSS molecules to the surface and interaction of the POSS molecules with each other through chemical condensation or physical aggregation. The appearance of aggregates on the surface of POSS-PI may be associated with the toughness deterioration of this sample, compared to PI, as will be further discussed.

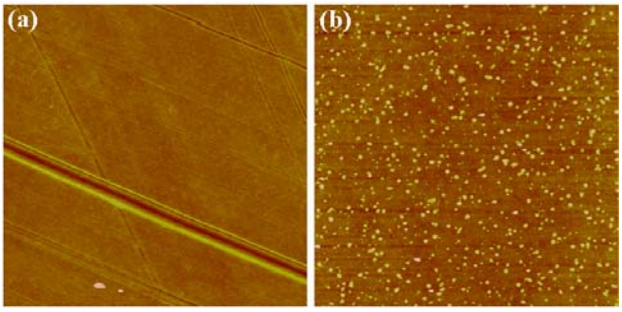


Fig. 7. AFM images of pristine PI (a) and 15 wt.% POSS-PI films (b). Scan size: 5×5 μm, z-range: 25 nm.

A further support for the suggested POSS aggregation in the 15 wt.% POSS-PI sample can be found in Fig. 8, where PI (Fig. 8a) and 15 wt.% POSS-PI (Fig. 8b) thin films were fractured under mode III, out-of-plane shearing, and investigated using high-resolution SEM (HRSEM).

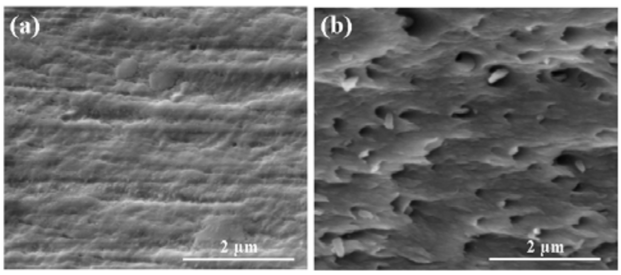


Fig. 8. HRSEM images of the fracture surfaces of PI (a) and 15 wt.% POSS-PI films (b). The fracture surfaces were obtained using a mode III, out-of-plane shearing.

The fracture surface of the PI thin film is smooth, showing no irregular features. The fracture surfaces of the 15 wt.% POSS-PI film is characterized by the formation of voids around aggregates, demonstrating the ability of the POSS aggregates to debond and to be pulled out of the PI matrix. The formation of voids around the POSS aggregates and the concentration of these voids play an important role in understanding the differences between the mechanical properties of the PI and POSS-PI.

Recalling the difference in the fracture surfaces, which were obtained during hypervelocity impacts (see Fig. 4), it can be deduced that debonding of aggregates during the impact of 15 wt.% POSS-PI sample is the cause for its spongy-like appearance, as will be further discussed.

### 3.3 POSS-PI nanostructure - failure model

Fig. 9 shows a schematic model for the PI (Fig. 9a) and 15 wt.% POSS-PI (Fig. 9b) fracture modes. Ojeda and Martin [21] have shown that the morphology of PMDA-ODA PI consists of spherulitic bundles of well-defined lamellae, similar to that typically observed in semicrystalline polymers. The lamellar crystal thickness was found to be 5-15 nm, corresponding to six PMDA-ODA repeat units along the chain axis [21], as illustrated schematically in Fig. 9.

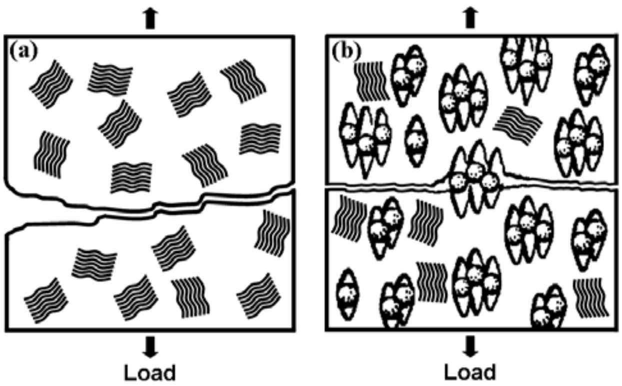


Fig. 9. Schematic presentation of the fracture modes of PI and 15 wt.% POSS-PI.

While applying tensile load on the PI film, the polymer is plastically deformed. Chain movement is initiated mainly between the crystalline lamella structures, were the mobility of the chains is higher. Initiation of fractures will occur at the edge of the sample at a random micro-crack, where the stresses concentrations are the highest.

Beside lamella structures, Fig. 9b also shows the POSS aggregates. Based on existing theories [22, 23], the effect of the aggregates' diameter, density and inter-aggregate distance on the mechanical properties of the 15 wt.% POSS-PI is defined as follows. While applying load, e.g. during tensile test, the POSS aggregates debond from the PI matrix, leading to the formation of voids around the aggregates as the polymer is plastically deformed. The small inter-aggregate distance and large aggregate diameter lead to lateral coalescence of the voids at early stages of the tensile test. This process is accompanied by high local stress acting on the thin ligaments between the aggregates. The lateral coalescence of the voids reduces the sample ability to withstand the stress loads. When the thin ligaments cannot support the load anymore, they fracture. Coalescence into critical-size voids may occur at any location along the gauge section, as shown in Fig. 9b.

The formation of voids around the POSS aggregates and the concentration of these voids play an important role in understanding the differences in the mechanical response of POSS-PI compared to PI during the hypervelocity impacts (see Fig. 3 and 4). Susceptibility of the 15 wt.% POSS-PI film to shearing at a temperature of -60°C is straightforward, and can be explained by the lower degree of chain mobility on one hand, and by the higher stress concentrations that are formed around debonded sites of the POSS aggregates, on the other hand. The shearing of the 15 wt.% POSS-PI film at 100°C is somewhat less expected. A possible explanation is that at 100°C, the temperature that is developed during the hypervelocity impact, along with the applied heat, allows higher chain mobility, which leads to a faster coalescence of the voids that were formed at debonded sites. The coalescence of the voids encourages the shearing of the film under impact at various locations, thus resulting in a large perforated area.

## 4. SUMMARY AND CONCLUSIONS

Film samples with POSS contents of 0 (PI) and 15 wt.%. POSS-PI were produced by a bench-scale process of casting and curing a pre-mixed solution of polyamic acid and POSS in N-methyl-pyrrolidone (NMP) solvent. The samples were produced in the form of thin films, 25–30 µm thick.

AFM and HRSEM results revealed the formation of POSS aggregates. The mechanical properties and fracture mechanism of 15 wt.% POSS-PI were shown to be dependent on the formation of these POSS aggregates. FTIR spectroscopy indicates that formation of aggregates was through physical aggregation or Si-O-Si networking, which occurs during the curing process at elevated temperature of the 15 wt.% POSS-PI.

A model demonstrating the effect of the POSS content on the POSS-PI mechanical properties was suggested. This model is based on voids formation around the aggregates during tensile tests, and coalescence of the voids if their diameter, distance and density are above a critical value.

The large amount of aggregates in the 15 wt.% POSS-PI films leads to increased brittleness of this material compared to PI under the same hypervelocity impact conditions. The shearing and radial cracking, which were formed in the 15 wt.% POSS-PI film during hypervelocity impacts, are attributed to the low toughness and elongation of the 15 wt.% POSS-PI. These properties change is related to formation of stress concentrations around the aggregates during the debonding process. In the case of PI, its toughness and elongation due to the absence of aggregates results in perforated area formation without any radial cracking, either at relatively high or low impact velocities.

Susceptibility of the 15 wt.% POSS-PI film to shearing at a temperature of -60°C is explained by the lower degree of chain mobility on one hand, and by the higher stress concentrations on the other hand, which are formed around aggregates' debonded sites.

The shearing effect of the 15 wt.% POSS-PI film at 100°C under hypervelocity impact may be explained as follows: the elevated temperature allows higher chain mobility, which leads to a faster coalescence of the voids that were formed at debonded sites. As explained before, the coalescence of the voids encourages the shearing of the film under impact.

## 5. REFERENCES


1. Bedingfield K. L., Leach R. D., and Alexander M. B., Spacecraft system failures and anomalies attributed to the natural space environment, *NASA Reference Publication 1390*, 1996.
2. Tribble A. C., *The space environment: Implementation for spacecraft design*, Princeton, New Jersey: Princeton University Press, 1995.
3. Grossman E., and Gouzman I., Space environment effects on polymers in low earth orbit, *Nucl. Instr. Meth. B*, Vol. 208, 48-57, 2003.
4. Connell J. W., and Watson K. A., Space environmentally stable polyimides and copolyimides derived from bis(3-aminophenyl)-3,5-di(trifluoromethyl)phenylphosphine oxide, *High Performance Polymers*, Vol. 13, no. 1, 23, 2001.
5. Verker R., Grossman E., Gouzman I., and Eliaz N., Residual stress effect on degradation of polyimide under simulated hypervelocity space debris and atomic oxygen, *Polymer*, Vol. 48, no. 1, 19, 2007.
6. Degroh K. K., and Banks B. A., Atomic-Oxygen Undercutting of Long-Duration Exposure Facility Aluminized-Kapton Multilayer Insulation, *Journal of Spacecraft and Rockets*, Vol. 31, no. 4, 656-664, 1994.
7. Boo W. J., Liu J., and Sue H. J., Fracture behaviour of nanoplatelet reinforced polymer nanocomposites, *Materials Science and Technology*, Vol. 22, no. 7, 829-834, 2006.
8. Brunsvold A. L., Minton T. K., Gouzman I. *et al.*, An investigation of the resistance of polyhedral oligomeric silsesquioxane polyimide to atomic-oxygen attack, *High Performance Polymers*, Vol. 16, no. 2, 303-318, 2004.
9. Gilman J. W., Schlitzer D. S., and Lichtenhan J. D., Low earth orbit resistant siloxane copolymers, *Journal of Applied Polymer Science*, Vol. 60, no. 4, 591, 1996.
10. Gonzalez R. I., Synthesis and *in-situ* Atomic Oxygen Erosion Studies of Space Survivable Hybrid Organic/Inorganic Polyhedral Oligomeric Silsesquioxane Polymers, Ph.D. Thesis, *Department of Chemical Engineering*, University of Florida, 2002.
11. Verker R., Grossman E., Gouzman I., and Eliaz N., POSS-polyimide nanocomposite films: Simulated hypervelocity space debris and atomic oxygen effects, *High Performance Polymers*, Vol. 20, no. 4-5, 475-491, 2008.
12. Du-Pont. Inc., Technical Bulletin, "PYRALIN® Polyimide Coating PI 2545 PI 2540 Product Information", February 1993.
13. Roybal R., Shively J., Stein C., and Tolmak P., *Cost Effective Testing for the 21st Century: Proc. 19th Space Simulation Conf.*, Baltimore, MD, USA, October 29-31, 1996.
14. Roybal R., Tlomak P., Stein C., and Stokes H., Simulated space debris impact experiments on toughened laminated thin solar cell cover glass, *International Journal of Impact Engineering*, Vol. 23, no. 1 pt 2, 811, 1999.
15. Tighe A., Gabriel S., and Van Eesbeek M., *Materials in Space Environment: Proc. of the ESA 8th Inter. Symp.*, Arcachon, France, 5-9 June, 2000.
16. Eliezer S., *The Interaction of High-Power Lasers with Plasmas*, Bristol: Institute of Physics, 2002.
17. Verker R., Eliaz N., Gouzman I. *et al.*, The effect of simulated hypervelocity space debris on polymers, *Acta Materialia*, Vol. 52, no. 19, 5539-5549 2004.
18. Callister W. D., *Material science engineering* New York: John Wiley & Sons, 2000.
19. Zhao Y. Q., and Schiraldi D. A., Thermal and mechanical properties of polyhedral oligomeric silsesquioxane (POSS)/polycarbonate composites, *Polymer*, Vol. 46, no. 25, 11640-11647, 2005.
20. Eon D., Raballand V., Cartry G. *et al.*, Plasma oxidation of polyhedral oligomeric silsesquioxane polymers, *J. Vac. Science Technol. B*, Vol. 24, no. 6, 2678-2688, 2006.
21. Ojeda J. R., and Martin D. C., High-Resolution Microscopy Of Pmda-Oda Poly(Imide) Single-Crystals, *Macromolecules*, Vol. 26, no. 24, 6557-6565, 1993.
22. Li J. X., Hiltner A., and Baer E., Fractography And Failure Mechanisms of Particulate-Filled Thermoplastic Polyester, *J. Applied Polymer Science*, Vol. 52, no. 2, 269-283, 1994.
23. Reynaud E., Jouen T., Gauthier C. *et al.*, Nanofillers in polymeric matrix: a study on silica reinforced PA6, *Polymer*, Vol. 42, no. 21, 8759-8768, 2001.